

Novel nanoliposomes for targeted codelivery of three anticancer agents against head and neck squamous cell carcinoma

Maryam Mohammadi¹, Fahimeh Bagheri Tofghi², Maedeh Vakili Saatloo³, Mehdi Talebi⁴,
 Maryam Kouhsoltani^{2,*}, and Hamed Hamishehkar^{5,6,*}

¹Department of Food Science and Engineering, Faculty of Agriculture, University of Kurdistan, Sanandaj, Iran.

²Department of Oral and Maxillofacial Pathology, Faculty of Dentistry, Tabriz University of Medical Sciences, Tabriz, Iran. ³Department of Periodontology, Henry M. Goldman School of Dental Medicine, Boston University, MA, USA.

⁴Emergency and Trauma Care Research Center, Tabriz University of Medical Sciences, Tabriz, Iran. ⁵Drug Applied Research Center, Tabriz University of Medical Sciences, Tabriz, Iran. ⁶New Material and Green Chemistry Research Center, Khazar University, Baku, Azerbaijan.

Abstract

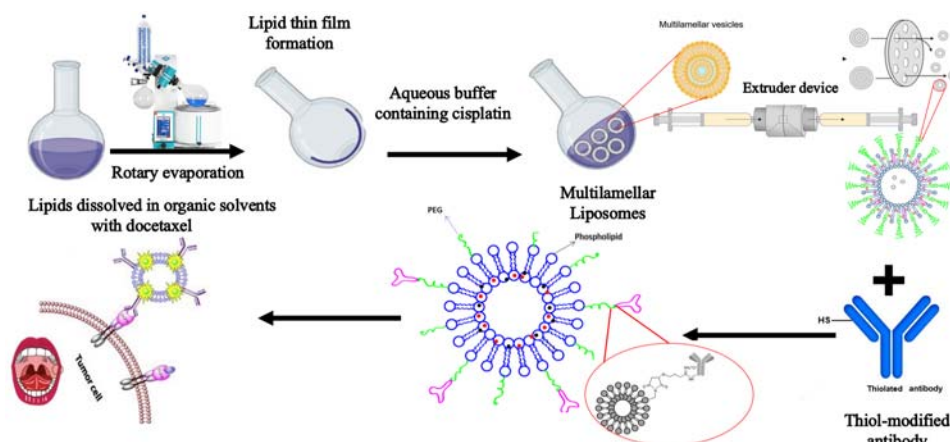
Background and purpose: Head and neck squamous cell carcinoma (HNSCC) is a malignant tumor in which the overexpression of epidermal growth factor receptor (EGFR) is associated with malignancy. For the treatment of HNSCC, cetuximab (CIT) as an anti-EGFR antibody is prescribed in combination with anticancer chemotherapy drugs for greater effectiveness.

Experimental approach: In this work, a CIT-targeted immunoliposome loaded with cisplatin (CP) and docetaxel (DTX) was developed to allow co-administration of the antibody and the anticancer chemotherapy drugs and selective delivery to HNSCC cells. Developed immunoliposomes were characterized for particle sizes, PDI, zeta potential, surface morphologies, and encapsulation efficiency. Moreover, additional *in vitro* studies were conducted, including cytotoxicity against HN5 cell line, and cellular uptake studies.

Findings/Results: The final targeted liposomes exhibited an average diameter of 68.65 ± 3.4 nm; PDI and zeta-potential were respectively around -7.9 ± 1.7 mV and 0.35 ± 0.05 . The encapsulation efficacy of DTX and CP within the immunoliposomes was approximately $95 \pm 4\%$ and $85 \pm 4\%$, respectively. Flow cytometric analysis revealed that the cellular uptake rate of final immunoliposomes was significantly higher than that of the naked liposomes, indicating that CT conjugation on the surface of nanoliposomes facilitated higher accumulation *via* receptor-mediated endocytosis. Moreover, co-encapsulation of CP and DTX into CIT-immunoliposomes increased the apoptosis by 24.06% compared to single-drug nanoformulations.

Conclusions and implications: The results indicated that nanoliposomes anchored with CIT enhanced drug accumulation and cytotoxicity in cancer cells and reduced the likelihood of adverse side effects, paving the way for more effective cancer therapies.

Keywords: Cisplatin; Docetaxel; Head and neck squamous cell carcinoma; Immunoliposomes; Targeted drug delivery.



*Corresponding authors:

M. Kouhsoltani, Tel: +98-4133355965, Fax: +98-4133346977

Email: koohsoltanim@tbzmed.ac.ir

H. Hamishehkar, Tel: +98-4133378163, Fax: +98-4133363311

Email: hamishehkar.hamed@gmail.com, hamishehkarh@tbzmed.ac.ir

Access this article online



Website: <http://rps.mui.ac.ir>

DOI: 10.4103/RPS.RPS_54_24

INTRODUCTION

Head and neck squamous cell carcinoma (HNSCC) presents a complex spectrum of diseases, encompassing tumors originating in various regions such as the lip/oral cavity, hypopharynx, oropharynx, nasopharynx, or larynx, each characterized by distinct epidemiological profiles, etiologies, and therapeutic challenges. Despite advancements in surgical, chemotherapy, and radiation treatments, HNSCC remains a significant health concern globally, ranking as the sixth most common malignancy and accounting for approximately 6% of all cancer cases, with an estimated 1-2% of cancer-related deaths (1). In the United States alone, an estimated 73,080 new cases were projected in 2020 (2). Despite therapeutic innovations, survival rates for HNSCC patients have stagnated over recent decades, primarily due to high rates of locoregional recurrence and distant metastasis (3). Conventional treatments, notably radiotherapy and chemotherapy, often lack specificity and are associated with considerable side effects and drug resistance, compromising treatment efficacy (4). Chemotherapy, a cornerstone in cancer therapy, frequently employs polypharmacy strategies to enhance efficacy and overcome multidrug resistance (MDR) (5). However, resistance development during treatment and adverse effects pose significant challenges to a successful outcome (6,7).

A key innovation in cancer therapy is the development of co-delivery systems that allow for the simultaneous delivery of multiple agents with complementary mechanisms of action. Such systems aim to maximize therapeutic efficacy by overcoming drug resistance and promoting synergistic effects on cancer cells (8,9). However, achieving effective co-delivery is technically challenging, particularly when combining agents with diverse pharmacokinetics and cellular uptake pathways (4). Among the well-established chemotherapeutic agents, cetuximab (CIT), docetaxel (DTX), cisplatin (CP), and methotrexate (MTX) offer unique anticancer mechanisms; CIT targets epidermal growth factor receptor (EGFR) to inhibit cancer cell proliferation and angiogenesis (10). By

targeting EGFR, CIT disrupts signaling cascades involved in cancer cell proliferation, invasion, and angiogenesis, with relatively mild side effects compared to traditional chemotherapeutic agents (11). DTX inhibits microtubule mobility, leading to cell mitotic arrest, while CP induces DNA damage, mainly through intra-strand cross-links, resulting in apoptotic cell death (12-14). Nanotechnology-based approaches, particularly lipid-based nanoparticles such as liposomes, provide a novel solution to these challenges. Liposomes offer enhanced permeability retention effects, facilitating targeted delivery to tumor sites. In this study, we introduce an innovative CIT-decorated liposome (immunoliposome) designed for the co-delivery of DTX and CP, providing targeted, dual-drug therapy directed at HNSCC cells (15,16). By combining these agents within an immunoliposome functionalized with CIT, our approach enhances cellular uptake and amplifies anticancer efficacy while reducing off-target effects. This unique triple-targeting system represents a significant advancement in co-delivery methodologies, improving therapeutic outcomes for HNSCC patients by enhancing specificity and minimizing side effects (17).

This study introduces a novel approach utilizing CIT-decorated immunoliposomes loaded with DTX and CP (IL CP/DTX). We evaluate the efficacy of this multi-drug formulation (IL CP/DTX) against HNSCC cells (HN-5) through *in vitro* cytotoxicity assays and apoptosis assessments. This novel formulation is expected to address the limitations of conventional therapies by offering a multi-faceted approach that enhances treatment specificity, effectiveness, and safety.

MATERIALS AND METHODS

Materials

Annexin-V/propidium iodide (PI), CP, cholesterol (Chol), CIT, fetal bovine serum (FBS), RPMI1640, trypsin 0.25%, penicillin/streptomycin (100X), (3-(4,5-dimethylthiazol-2-yl)-2,5-diphenyltetrazolium bromide (MTT), N-succinimidyl-S-acetylthioacetate (SATA), ethylenediaminetetraacetic acid (EDTA), bovine serum albumin (BSA), and dimethyl sulfoxide

(DMSO) were acquired from Sigma Aldrich (Hamburg, Germany). DTX was purchased from Arasto Pharmaceutical Chemicals Inc. (Saveh, Iran). Cell culture materials were procured from Gibco Co. (UK). Distearoylphosphatidylethanolamine-poly(ethylene glycol) (DSPE-PEG) (2000) Maleimide, and mPEG (2000) were obtained from Avanti Polar Lipids, Inc. (Birmingham, AL).

Preparation of nanoliposomes

Unilamellar liposomes were prepared using the thin-layer hydration-extrusion method (18). A lipid mixture consisting of soybean lecithin/Chol/mPEG2000-DSPE/Mal PEG2000-DSPE (60:40:2:0.5 mole ratio) was dissolved in chloroform, and 4 mg of DTX was added to the mixture.

The thin lipid film was rotaevaporated for 30 min and hydrated for 20 min using phosphate-buffered saline (PBS) pH 7.4 containing CP for a final concentration of 1000 µg/mL of the drug. The resulting multilamellar liposomes were extruded five times through a polycarbonate membrane with a pore size of 100 nm by an extrusion machine to obtain unilamellar nanoliposomes (Tabriz, Iran).

Preparation steps of thiolated CIT

CIT (5 mL, 1.5 mL containing 7.5 mg drug) was transferred to the upper section of an Amicon filter (molecular cut-off 100 kD, Millipore Sigma, Burlington, MA) and washed with diluted PBS ten times to remove glycine amino acids. Forty microliters of SATA dissolved in DMSO were added to the mixture and stirred for 2 h at 4 °C. The solution was washed with PBS ten times to remove unreacted SATA.

Seventy milligrams of hydroxylamine and 14.6 mg of EDTA were dissolved in 1 mL of PBS, and 250 µL of the mixture was added to CIT containing SATA under a nitrogen atmosphere. Unreacted hydroxylamine and EDTA were removed by washing the solution with PBS ten times.

Development of immunoliposomes

Eight hundred microliters of the thiolated solution were added to the liposomal suspension and stirred for 4 h at 4 °C. The thiol groups act as a crosslinker with the maleimide

groups of the DSPE-PEG2000-Mal lipid, forming a thioether bond. The final formulation was purified by ultrafiltration at 2200 g for 60 min using the filter Amicon with cut off 300000 kD, followed by a washout process with PBS to remove the non-bound ligand. To prevent particle aggregation, liposomes were incubated with 1 mM of l-cysteine, which blocks the free maleimide radicals, preventing the formation of a disulfide bond. The immunoliposome was stored at 4 °C until use (19).

Characterization of nanoliposomes

The particle size, polydispersity index (PDI), and zeta potentials of the prepared nanoliposomes were measured by dynamic light scattering (DLS; Zetasizer-ZS, Malvern, UK). The morphology of the synthesized nanoliposomes was studied *via* scanning electron microscopy (SEM; EM 3200, KYKY, China) and transmission electron microscopy (TEM; LEO 906, Zeiss, 100 kV, Germany).

Encapsulation efficiency

The unloaded DTX was separated by an Amicon filter (Ultra-0.5, Millipore, molecular cut-off 30 kD); for this process, 1 mL of the formulation was diluted with 1 mL ethanol 40%, and this mixture was heated and subjected to a sonication process. The resulting solution was poured into the upper chamber of the Amicon filter and centrifuged at 4000 rpm for 10 min. The solution gathered at the Amicon filter's bottom section was free DTX. High-performance liquid chromatography (HPLC) was used to investigate the unloaded DTX formulation. Chromatographic analyses were performed with a Knauer C18 column (Eurospher II, 10 µm, 250 × 4.6 mm, Berlin, Germany) and acetonitrile and water (45:55, v/v) as the mobile phase, which was pumped at a rate of 1 mL/min. The required wavelength was 230 nm (20). The unloaded CP was determined by Amicon Ultra-0.5 (Millipore, molecular cut-off 30 kD).

For this process, 1 mL of formulation was diluted with 1 mL of distilled water and the mixture was poured into the upper chamber of the Amicon filter and centrifuged at 4000 rpm for 10 min. The solution that was gathered at the bottom section of the Amicon filter was free CP and was determined at 310 nm using a spectrophotometer,

Ultrascope 2000® (Pharmacia Biotech, UK) (21). The encapsulation efficiency of the synthesized nanoliposomes was calculated using the following equation:

$$\text{Encapsulation efficiency (\%)} = \frac{\text{Total drug} - \text{free drug}}{\text{Total drug}} \times 100$$

To determine the coupling efficiency of CIT, 1 mL of formulation was diluted with distilled water and centrifuged at 80000 rpm for 30 min using the ultracentrifuge. A Bradford protein assay determined the unbound CIT amount in the supernatant solution. BSA was used as a standard protein to plot a calibration curve.

Cell culture

Human head and neck squamous cell carcinoma (HN5) cells were obtained from the National Cell Bank of Iran, Pasteur Institute (NCBI), and cultured in RPMI 1640 supplemented with 10% FBS, penicillin, and streptomycin at 37 °C in 5% CO₂ and 95% air with more than 95% humidity.

In vitro cytotoxicity

The biocompatibility and cytotoxicity of the IL CP/DTX were assessed by MTT assay on the HN5 cell line. Cells were seeded into a 96-well plate and treated with a medium containing various concentrations of the IL CP/DTX, and blank liposomes for 48 h. The optical density values were measured at 570 nm with a microplate reader (Elx808, Biotek, Winooski, VT). The combination index was estimated to assess the synergistic effect based on IC₅₀ values acquired from individual drugs alone and combination treatment (22).

In vitro cellular uptake

Flow cytometry analysis was used to estimate the cellular uptake of immunoliposomes against HN5 cell line. Rhodamine B (RhB) was used as a fluorescent agent for its fluorescent properties. Cells were seeded in six-well plates, treated with single liposomes loaded with RhB (LRhB) and immunoliposomes loaded with RhB (ILRhB), and incubated. After 2, 4, 8, 12, 24, and 48 h, cellular uptake was evaluated based on RhB fluorescence using a FACS Calibur flow cytometer.

In vitro cell apoptosis

Annexin V/PI double staining assay

Apoptosis-mediated cell death of tumor cells was studied using FITC-labeled Annexin V/PI according to the manufacturer's protocol (23). HN5 cell line (2-3 × 10⁵ cells/well) was incubated at 37 °C with 5% CO₂ for 24 h in the presence of the mixture of L CIS/DTX and IL CIS/DTX. Untreated cells were used as a control. Cells were trypsinized, washed twice with cold PBS, and centrifuged for 5 min at 3000 rpm. After removal of the supernatants, the cells were resuspended in 100 μL Annexin V binding buffer and then incubated for 20 min in 5 μL of annexin V FITC. PI solution (5 μL, 1 mg/mL) was added to each cell. The apoptotic cells were specified and analyzed by a FACS Calibur flow cytometer.

Statistical analysis

Each experiment was repeated three times, and the mean and standard deviation were calculated. A two-way ANOVA followed by Tukey's post hoc test was used to assess the main effects of treatment concentration and drug type, as well as their interaction on cell viability using GraphPad Prism version 9.0.2 (San Diego, CA, USA). A *P*-value < 0.05 was considered statistically significant.

The independent t-tests were used for the *in vitro* cellular uptake and cell viability between L CP: DTX (1:2), and IL CP: DTX (1:2).

RESULTS

Preparation and characterization of nanoliposomes

Nanoliposomes were successfully fabricated using the thin-film hydration-extrusion technique. The characterization data for different formulations showed a narrow size distribution and negative zeta potential for all prepared formulations. According to Fig. 1A, before CIT coupling, the liposomes exhibited a mean diameter of 58.56 ± 4.2 nm and a PDI of 0.28 ± 0.03, indicating a uniform particle distribution. Following CIT attachment, a slight increase in size and PDI was observed, with the size increasing to 68.65 ± 3.4 nm and the PDI to 0.35 ± 0.05 (Fig. 1A). The zeta potential for blank liposomes was -17.7 ± 0.9 mV, which increased to -7.99 ± 1.7 mV after CIT coupling (Fig. 1B).

SEM images revealed particles with sizes under 100 nm, homogenous distribution, and spherical morphology (Fig. 1C). TEM images corroborated these findings, showing predominantly spherical particles with a bilayer structure (Fig. 1D). The encapsulation efficacy of DTX and CP within the immunoliposomes was approximately $95 \pm 4\%$ and $85 \pm 4\%$, respectively. Bradford's assay was successfully performed to confirm the

conjugation of CT on the liposome surface. Bradford's assay is a colorimetric method to estimate the protein content in a sample. Quantitative estimation of CT, using BSA as a standard, was done to calculate the amount of protein conjugated on the surface of freshly prepared nanoliposomes. The results showed that the degree of conjugation of CT to the nanoliposome surface was 90.5%.

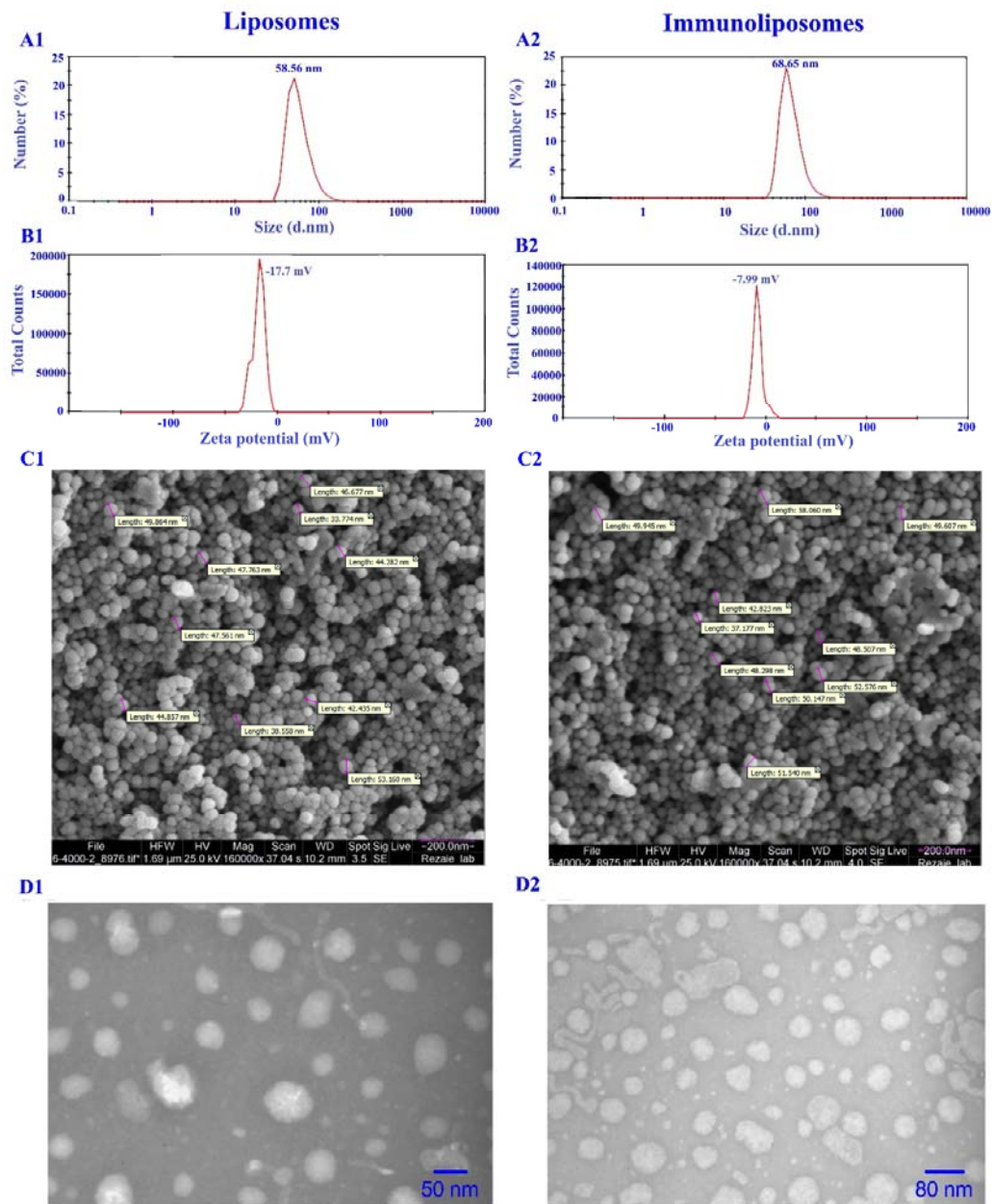


Fig. 1. Characterization of prepared liposomes (1) and immunoliposomes (2) showing: (A) size distribution, (B) zeta potential, (C) scanning electron microscopy (SEM) image, and (D) transmission electron microscopy (TEM) image.

Cellular uptake

The quantitative cellular uptake of LRhB and ILRhB was determined via flow cytometric analysis on HN5 cells. Figure 2 shows a time-dependent cell uptake. The fluorescent intensity of cells treated with ILRhB was significantly higher than that of cells treated with LRhB.

Cell cytotoxicity and cell apoptosis

In the first phase of the experiment, the effect of co-delivering CP and DTX on HNSCC cancer was measured using the MTT assay. This test assessed the cytotoxic effects of L CP, L DTX, and L CP/DTX at ratios of 1:1, 1:2, and 1:4, and IL CP/DTX on HN-5 cell viability. After 48 h of treatment, cell viability significantly decreased. IC₅₀ values for L CP and L DTX were estimated to be 22.63 and 11.59 μM, respectively (Fig. 3A). To determine the optimal combinational ratio of CP and DTX in liposomal formulations, IC₅₀ values were measured, revealing values of 7.59, 5.53, and 9.93 μM at ratios of 1:1, 1:2, and 1:4, respectively. The evaluation of immune targeting effects on cell cytotoxicity efficacy

showed a decrease in IC₅₀ from 5.53 to 3.83 μM for IL CP/DTX at the optimal 1:2 ratio (Fig. 3B).

In the second phase of the experiment, the effect of the prepared samples on the activation of apoptosis pathways and DNA fragmentation was measured using the annexin V/PI staining technique. Apoptosis was quantitatively assessed by staining HN-5 cells with annexin V/PI following treatment with CP, DTX, L CP/DTX (1:2), and IL CP/DTX for 48 h, with blank liposomes serving as a negative control. HN-5 cells treated with blank liposomes exhibited negligible apoptosis. Apoptosis rates of 16.6%, 25.0%, and 29.3% were observed for free L CP, L DTX, and L CP/DTX (1:2), respectively, compared to blank liposomes (control group). Furthermore, the apoptosis rate for IL CP/DTX was 47.7%. Co-encapsulation of CP, DTX, and CIT increased the apoptosis rate by 24.06% compared to individual drug formulations, highlighting the efficacy of IL CP/DTX nanoparticles in inducing higher apoptosis than single-drug-loaded nano formulation and non-targeted nanoparticles (Fig. 4).

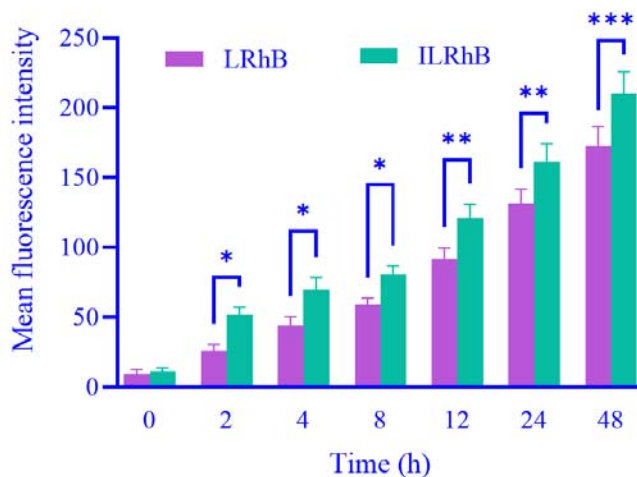


Fig. 2. Cellular uptake of LRhB and ILRhB reveals the apoptotic effects and nuclear changes induced by the formulations. **P* < 0.1, ***P* < 0.01, ****P* < 0.001 indicate the significant differences between the designated groups. LRhB, Liposomes loaded with Rhodamine B; ILRhB, immunoliposomes loaded with Rhodamine B. Data are expressed as mean ± SD (n = 3)

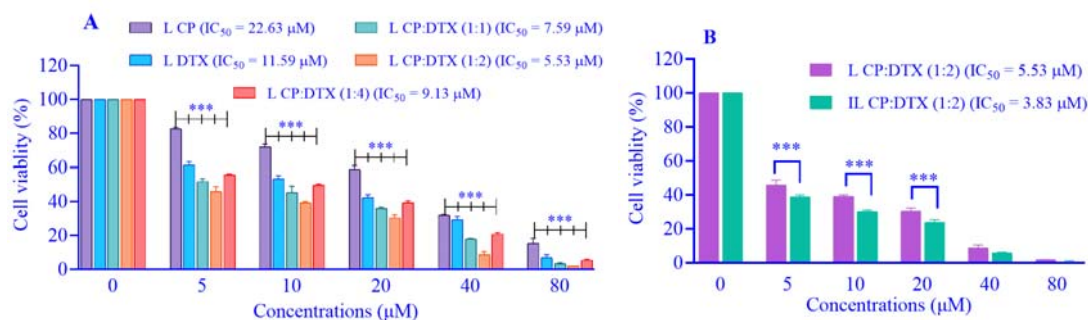


Fig. 3. Cell toxicity of CP and DTX as (A) single-drug nanoformulations and (B) co-formulated non-targeted and targeted IL against head and neck squamous cell carcinoma (HN-5). Data are presented as mean \pm SD, n = 3; CP, Cisplatin; DTX, docetaxel; L, liposome; IL, immunoliposome.

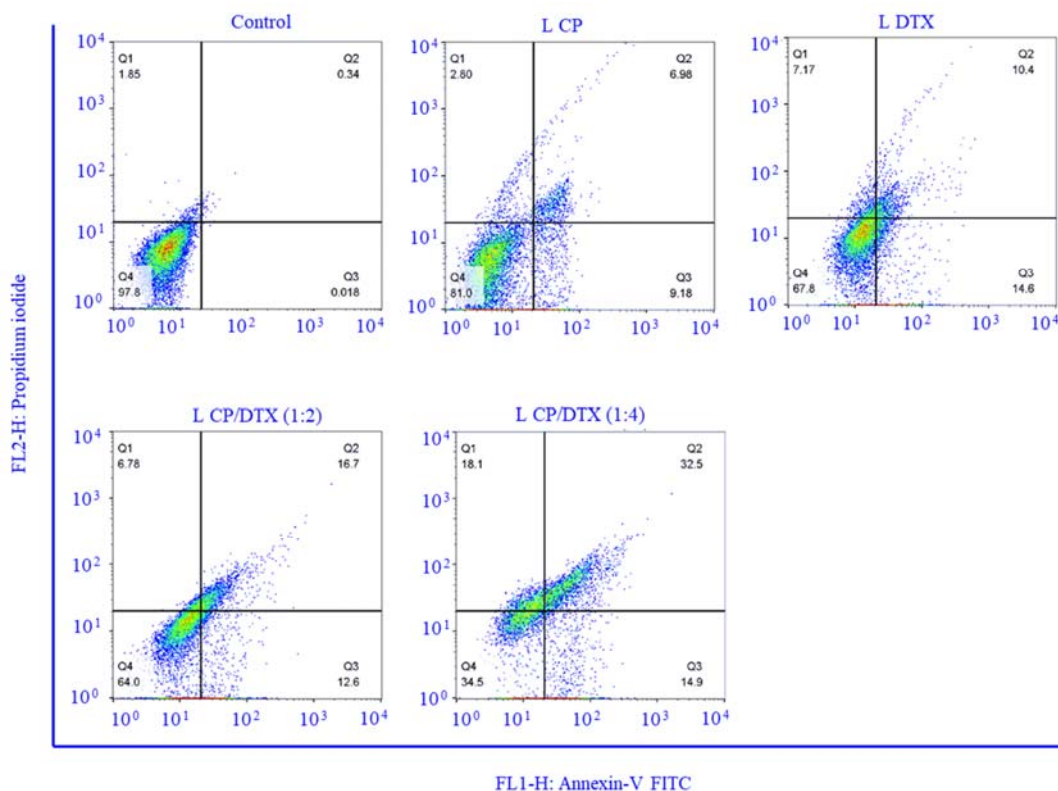


Fig. 4. Evaluation of apoptosis in HN-5 cells treated with blank liposomes (serve as control group), liposomal cisplatin (L CP), liposomal docetaxel (L DTX), liposomal co-formulation of docetaxel and cisplatin (L CP:DTX 1:2), and immunoliposomes of docetaxel and cisplatin (IL CP:DTX).

DISCUSSION

The current study demonstrates the successful preparation and characterization of nanoliposomes and immunoliposomes for the targeted co-delivery of CP and DTX to HNSCC. Utilizing the thin-film hydration-extrusion technique, we achieved a robust nanoformulation with a mean diameter of 58

nm and a relatively uniform particle distribution (PDI of 0.28). Post-CIT attachment, the particle size, and PDI increase confirmed successful conjugation, which is essential for enhanced cellular interaction and stability in biological environments. The thiol groups of CIT act as a crosslinker with the maleimide groups of the DSPE-PEG2000-Mal lipid, forming a thioether bond. The zeta potential shift observed in our

study, from -17.7 mV to -7.99 mV post-CIT attachment, is consistent with reports by Khashayar *et al.*, who found that antibody conjugation increases the zeta potential, improving nanoparticle stability and cellular uptake (24). The positive shift in zeta potential after CIT coupling confirms the successful presentation of CIT on the surface of nanoliposomes due to its positive charge at physiologic pH. The isoelectric point of CIT is 8.48. In another study, CIT attachment did not affect the main particle characteristics, as none of the assayed parameters reached a statistically significant difference among formulations (25). Petrilli *et al.* did not find any statistically significant differences in size and polydispersity between liposomes and immunoliposomes containing 5-FU. However, the coupling of CIT to obtain immunoliposomes slightly decreased the zeta potential of the dispersion (26).

The high encapsulation efficiency for both DTX ($95 \pm 4\%$) and CP ($85 \pm 4\%$) within the immunoliposomes underscores the potential of these nanocarriers to deliver a substantial payload to cancer cells. These values are comparable to those reported by Pakdaman Goli *et al.*, who achieved encapsulation efficiencies of 99.6% for gemcitabine and 91% for CP in similar liposomal formulations, indicating the robustness of our encapsulation method (27). In another study, the encapsulation efficiency obtained for the hydrophilic anticancer drug (5-FU) into liposomes and immunoliposomes was 45.8 ± 2.0 and 44.1 ± 2.6 , respectively (26). The high encapsulation efficiency for CP in this study could be due to the appropriateness of the ratios of liposome ingredients used and the effectiveness of the applied method. Flow cytometric analysis revealed a significantly higher cellular uptake of ILRhB compared to LRhB, demonstrating the enhanced targeting capability conferred by cetuximab conjugation.

This greater uptake of the immunoliposomes is likely due to endocytosis mediated through the interaction between CIT and EGFR. This targeted delivery is crucial for maximizing therapeutic efficacy while minimizing off-target effects. Our results are in agreement with those of Yue *et al.*, indicating that CIT-

conjugated liposomes exhibited significantly higher cellular uptake and cytotoxicity in EGFR-positive cancer cells compared to non-targeted liposomes (28). In another study, encapsulation of oxaliplatin into CIT-immunoliposome improved its pharmacokinetics, allowing a more selective and efficient internalization of liposomes and delivery to the tumor (25). It has been demonstrated that CIT-conjugated liposomes significantly enhanced the delivery and efficacy of 5-FU in skin squamous carcinoma cells, corroborating our findings of improved cellular uptake and cytotoxicity in HNSCC cells (29).

Cytotoxicity assays conducted on HN-5 cells using the MTT assay showed that the co-delivery of CP and DTX significantly reduced cell viability, with IL CP demonstrating superior efficacy over non-targeted formulations. The IC_{50} value for IL CP/DTX was markedly lower at the optimal 1:2 ratio, highlighting the synergistic effect of the co-delivery system. This significantly improved cytotoxicity may be attributed to the small size of the prepared particles, their ability to undergo cellular uptake, and the improvement in the intracellular concentration of anticancer chemotherapy drugs. This finding is consistent with studies conducted by Asadollahi *et al.*, which reported enhanced cytotoxicity and reduced IC_{50} values for targeted co-delivery of chemotherapeutic agents in nanoformulations (20). In another study, CIT-targeted liposomes containing oxaliplatin decreased IC_{50} values 2-4 fold in HT-29 and SW-480, which demonstrated significant resistance to free oxaliplatin, reaching nearly similar efficacy as in the more sensitive HCT-116 cells (25). In another study, the folate-decorated biodegradable poly (lactide-co-glycolide) (PLGA) nanoparticles were developed for tumor targeting of anticancer agents. Due to the overexpression of the folate receptor on tumor surface, folate has been efficiently employed as a targeting moiety for various anticancer agents to avoid their non-specific attacks on normal tissues and also to increase their cellular uptake within target cells. The average size and encapsulation efficiency of the prepared PLGA-folate nanoparticles were found to be around 115 ± 12 nm and 57%, respectively. The

in vitro intracellular uptakes of PLGA-folate nanoparticles showed greater cytotoxicity on cancer cell lines compared to non-folate mediated carriers (30). In another study, DTX was encapsulated into anti-EGFR immunoliposomes. The prepared formulations were nanosized, with high drug encapsulation and controlled release. Immunoliposomes showed higher uptake by EGFR-expressing cells. Moreover, immunoliposomes were more cytotoxic to prostate cancer EGFR-expressing cells (31).

The apoptosis assays revealed that co-encapsulation of CP and DTX in immunoliposomes (IL CP/DTX) significantly increased apoptosis rates compared to individual drug formulations and non-targeted nanoparticles. The apoptosis rate of 47.7% for IL CP/DTX is particularly notable, indicating that the immunoliposome formulation enhances the pro-apoptotic effects of the drugs. This enhanced apoptosis can be attributed to improved drug accumulation in the cancer cells and more effective disruption of cellular processes, as similarly reported by Dianat-Moghadam *et al.* in their study on targeted liposomal drug delivery systems (32). In another study, drug delivery strategies based on receptor targeting with novel ligand-anchored carriers exploiting CD44, folate, and integrin $\alpha V\beta$ were reviewed, as well as toll-like receptors (TLRs) expressed on synovial monocytes and macrophages and antigen-presenting cells, for possible active targeting in rheumatoid arthritis. They concluded that common conventional receptors and multifunctional ligands that are involved in targeting receptors or developing nanocarriers with appropriate ligands for TLRs could provide profound targeting drug delivery systems for the effective treatment of RA (33). In another study, targeted long-circulating immunoliposomes containing simvastatin (tLCLS) with an anti-EGFR antibody attached to their surface were obtained and proved effective in the treatment of an *in-vitro* model of triple-negative breast cancers. The conducted *in-vitro* experiments demonstrated that tLCLS treatment led to a decrease in membrane order and inhibited PI3K/Akt signalling to induce apoptosis.

The analyses of the efficacy of the tLCLS on the animal model indicated that immunoliposomes were effectively delivered to tumors (34).

Our study's findings suggest that CIT-conjugated nanoliposomes for the co-delivery of CP and DTX significantly enhance drug delivery efficiency and therapeutic efficacy against HNSCC. This targeted approach improves drug accumulation and cytotoxicity in cancer cells and reduces the likelihood of adverse side effects, paving the way for more effective cancer therapies. Future studies should focus on *in vivo* assessments to further validate the nanocarriers' therapeutic potential and safety. Additionally, exploring the mechanisms underlying the enhanced cellular uptake and apoptosis induction could provide deeper insights into optimizing these delivery systems for clinical applications.

CONCLUSIONS

In this work, a novel therapeutic for HNSCC treatment was investigated. IL CP/DTX showed homogeneously dispersed nanoparticles of nano-size range (68.65 ± 3.4 nm), and the zeta potential of the preparations was -7.99 ± 1.77 mV. The nanoparticles showed a significant increase in cellular uptake in the HN5 cell line as compared to naked liposomes. The resulting immunoliposomes potentially combine the therapeutic activity and selectivity of CIT with cancerous-cell delivery of immunoliposomes containing DTX and CP in a single therapeutic method. We expect that future clinical trials will confirm the potential of DTX and CP co-loaded into immunoliposomes against HNSCC tumors.

Acknowledgments

The research reported in this publication was supported by the Elite Researcher Grant Committee under award number 972648 from the National Institute for Medical Research Development (NIMAD), Tehran, Iran. We would like to express our appreciation for the cooperation of the Clinical Research Development Unit of Imam Reza General Hospital, Tabriz, Iran, in conducting this research.

Conflict of interest statement

The authors declared no conflict of interest in this study.

Authors' contributions

M. Mohammadi, F. Bagheri, and M. Talebi contributed to data curation, preparation, and writing of the original draft of the article; M. Kouhsoltani and H. Hamishehkar contributed to the conceptualization and supervision of the study. All authors have read and approved the finalized article. Each author has fulfilled the authorship criteria and affirmed that this article represents honest and original work.

Data availability statement

The data that support the findings of this study are available from the corresponding author upon reasonable request.

AI declaration

The authors did not use any AI-assisted technologies in the preparation of this manuscript

REFERENCES

1. Ferlay J, Shin HR, Bray F, Forman D, Mathers C, Parkin DM. Estimates of worldwide burden of cancer in 2008: GLOBOCAN 2008. *Int J Cancer*. 2010;127(12):2893-2917. DOI: 10.1002/ijc.25516.
2. Siegel RL, Miller KD, Jemal A. Cancer statistics, 2020. *CA Cancer J Clin*. 2020;70(1):7-30. DOI: 10.3322/caac.21590.
3. Fedele S. Diagnostic aids in the screening of oral cancer. *Head Neck Oncol*. 2009;1:5,1-6. DOI: 10.1186/1758-3284-1-5.
4. Zeinali M, Abbaspour-Ravasjani S, Ghorbani M, Babazadeh A, Soltanfam T, Santos AC, et al. Nanovehicles for co-delivery of anticancer agents. *Drug Discov Today*. 2020;25(8):1416-1430. DOI: 10.1016/j.drudis.2020.06.027.
5. Nanni O, Amadori D, De Censi A, Rocca A, Freschi A, Bologna A, et al. Metformin plus chemotherapy versus chemotherapy alone in the first-line treatment of HER2-negative metastatic breast cancer. The MYME randomized, phase 2 clinical trial. *Breast Cancer Res Treat*. 2019;174(2):433-442. DOI: 10.1007/s10549-018-05070-2.
6. Naghizadeh S, Mohammadi A, Baradaran B, Mansoori B. Overcoming multiple drug resistance in lung cancer using siRNA targeted therapy. *Gene*. 2019;714,1-11. DOI: 10.1016/j.gene.2019.143972.
7. Shi K, Xue B, Jia Y, Yuan L, Han R, Yang F, et al. Sustained co-delivery of gemcitabine and cisplatinum via biodegradable thermo-sensitive hydrogel for synergistic combination therapy of pancreatic cancer. *Nano Res*. 2019;12(6):1389-1399. DOI: 10.1007/s12274-019-2342-7.
8. Lages EB, Fernandes RS, Silva JDO, de Souza ÂM, Cassali GD, de Barros ALB, et al. Co-delivery of doxorubicin, docosahexaenoic acid, and α -tocopherol succinate by nanostructured lipid carriers has a synergistic effect to enhance antitumor activity and reduce toxicity. *Biomed Pharmacother*. 2020; 132:1-12. DOI: 10.1016/j.biopha.2020.110876.
9. Parhi P, Mohanty C, Sahoo SK. Nanotechnology-based combinational drug delivery: an emerging approach for cancer therapy. *Drug Discov Today*. 2012;17(17-18):1044-1052. DOI: 10.1016/j.drudis.2012.05.010.
10. Mahmoudi S, Ghorbani M, Sabzichi M, Ramezani F, Hamishehkar H, Samadi N. Targeted hyaluronic acid-based lipid nanoparticle for apigenin delivery to induce Nrf2-dependent apoptosis in lung cancer cells. *J Drug Deliv Sci Technol*. 2019;49:268-276. DOI: 10.1016/j.jddst.2018.11.013.
11. Gold KA, Lee HY, Kim ES. Targeted therapies in squamous cell carcinoma of the head and neck. *Cancer*. 2009;115(5):922-935. DOI: 10.1002/cncr.24123.
12. Herbst RS, Shin DM. Monoclonal antibodies to target epidermal growth factor receptor-positive tumors: a new paradigm for cancer therapy. *Cancer*. 2002;94(5):1593-1611. DOI: 10.1002/cncr.10372.
13. Imran M, Saleem S, Chaudhuri A, Ali J, Baboota S. Docetaxel: an update on its molecular mechanisms, therapeutic trajectory and nanotechnology in the treatment of breast, lung and prostate cancer. *J Drug Deliv Sci Technol*. 2020;60:1-18. DOI: 10.1016/j.jddst.2020.101959.
14. Dasari S, Tchounwou PB. Cisplatin in cancer therapy: molecular mechanisms of action. *Eur J Pharmacol*. 2014;740:364-378. DOI: 10.1016/j.ejphar.2014.07.025.
15. de Souza ALR, Amorim ACF, Cintra ER, Ferreira NN, Silva LAD, Hayasaki TG, et al. Development and validation of a rapid RP-HPLC method for simultaneous quantification of paclitaxel and cetuximab in immunoliposomes. *Talanta*. 2021;225:121988,1-30. DOI: 10.1016/j.talanta.2020.121988.
16. Zhang L, Shi J, Zhu MH, Huang Y, Lu Q, Sun P, et al. Liposomes-enabled cancer chemoimmunotherapy. *Biomaterials*. 2024:122801. DOI: 10.1016/j.biomaterials.2024.122801.
17. Portnoy E, Lecht S, Lazarovici P, Danino D, Magdassi S. Cetuximab-labeled liposomes containing near-infrared probe for *in vivo* imaging. *Nanomedicine*. 2011;7(4):480-488. DOI: 10.1016/j.nano.2011.01.001.
18. Mansoori B, Mohammadi A, Abedi-Gaballu F, Abbaspour S, Ghasabi M, Yekta R, et al. Hyaluronic

- acid-decorated liposomal nanoparticles for targeted delivery of 5-fluorouracil into HT-29 colorectal cancer cells. *J Cell Physiol.* 2020;235(10):6817-6830.
DOI: 10.1002/jcp.29576.
19. Pan X, Wu G, Yang W, Barth RF, Tjarks W, Lee RJ. Synthesis of cetuximab-immunoliposomes *via* a cholesterol-based membrane anchor for targeting of EGFR. *Bioconj Chem.* 2007;18(1):101-108.
DOI: 10.1021/bc060174r.
 20. Asadollahi L, Mahoutforoush A, Dorreyatim SS, Soltanfam T, Paiva-Santos AC, Peixoto D, *et al.* Co-delivery of erlotinib and resveratrol *via* nanostructured lipid carriers: a synergistically promising approach for cell proliferation prevention and ROS-mediated apoptosis activation. *Int J Pharm.* 2022;624:1-10.
DOI: 10.1016/j.ijpharm.2022.122027.
 21. Parhizkar F, Yousefi M, Soltani-Zangbar MS, Parhizkar Z, Aghabati-Maleki L, Abbaspour-Ravasjani S, *et al.* Sirolimus- and cyclosporine-loaded nanostructured lipid carriers: development, characterization, and *in vitro* evaluation in T-cell profiles of patients with a history of recurrent pregnancy loss. *Reprod Med Biol.* 2023;22(1):1-15.
DOI: 10.1002/rmb2.12509.
 22. Asghariazar V, Vahidian F, Karimi A, Abbaspour-Ravasjani S, Mansoori B, Safarzadeh E. The role of oleuropein, derived from olives, in human skin fibroblast cells: investigating the underlying molecular mechanisms of cytotoxicity and antioxidant and anti-inflammatory activities. *Int J Clin Pract.* 2024;2024:1-12.
DOI: 10.1155/2024/8827501.
 23. Mahoutforoush A, Asadollahi L, Hamishehkar H, Abbaspour-Ravasjani S, Solouk A, Nazarpak MH. Targeted delivery of pennyroyal *via* methotrexate functionalized PEGylated nanostructured lipid carriers into breast cancer cells; a multiple pathways apoptosis activator. *Adv Pharm Bull.* 2023;13(4):747-760.
DOI: 10.34172/apb.2023.077.
 24. Khashayar P, Amoabediny G, Larijani B, Hosseini M, Vanfleteren J. Fabrication and verification of conjugated AuNP-Antibody nanoprobe for sensitivity improvement in electrochemical biosensors. *Sci Rep.* 2017;7(1):1-8.
DOI: 10.1038/s41598-017-12677-w.
 25. Zalba S, Contreras AM, Haeri A, Ten Hagen TL, Navarro I, Koning G, *et al.* Cetuximab-oxaliplatin-liposomes for epidermal growth factor receptor targeted chemotherapy of colorectal cancer. *J Control Release.* 2015;210:26-38.
DOI: 10.1016/j.jconrel.2015.05.271.
 26. Pettrilli R, Eloy JO, Saggiaro FP, Chesca DL, de Souza MC, Dias MV, *et al.* Skin cancer treatment effectiveness is improved by iontophoresis of EGFR-targeted liposomes containing 5-FU compared with subcutaneous injection. *J Control Release.* 2018;283:151-162.
DOI: 10.1016/j.jconrel.2018.05.038.
 27. Pakdaman Goli P, Bikhof Torbati M, Parivar K, Akbarzadeh Khiavi A, Yousefi M. Preparation and evaluation of gemcitabin and cisplatin-entrapped folate-PEGylated liposomes as targeting co-drug delivery system in cancer therapy. *J Drug Deliv Sci Technol.* 2021;65:13-22.
DOI: 10.1016/j.jddst.2021.102756.
 28. Yue S, Zhang Y, Wei Y, Haag R, Sun H, Zhong Z. Cetuximab-polymersome-mertansine nanodrug for potent and targeted therapy of EGFR-positive cancers. *Biomacromolecules.* 2022;23(1):100-111.
DOI: 10.1021/acs.biomac.1c01065.
 29. Pettrilli R, Eloy JO, Lopez RFV, Lee RJ. Cetuximab immunoliposomes enhances delivery of 5-FU to skin squamous carcinoma cells. *Anticancer Agents Med Chem.* 2016;17(2):301-308.
DOI: 10.2174/1871520616666160526110913.
 30. Heidarian S, Derakhshandeh K, Adibi H, Hosseinzadeh L. Active targeted nanoparticles: preparation, physicochemical characterization and *in vitro* cytotoxicity effect. *Res Pharm Sci.* 2015;10(3):241-251.
PMID: 26600851.
 31. Eloy JO, Ruiz A, de Lima FT, Pettrilli R, Raspantini G, Nogueira KAB, *et al.* EGFR-targeted immunoliposomes efficiently deliver docetaxel to prostate cancer cells. *Colloids Surf B Biointerfaces.* 2020;194:111185,1-12.
DOI: 10.1016/j.colsurfb.2020.111185.
 32. Dianat-Moghadam H, Abbaspour-Ravasjani S, Hamishehkar H, Rahbarghazi R, Nouri M. LXR inhibitor SR9243-loaded immunoliposomes modulate lipid metabolism and stemness in colorectal cancer cells. *Med Oncol.* 2023;40(6):156.
DOI: 10.1007/s12032-023-02027-4.
 33. Emami J, Ansarypour Z. Receptor targeting drug delivery strategies and prospects in the treatment of rheumatoid arthritis. *Res Pharm Sci.* 2019;14(6):471-487.
DOI: 10.4103/1735-5362.272534.
 34. Matusiewicz L, Filip-Psurska B, Psurski M, Tabaczar S, Podkalicka J, Wietrzyk J, *et al.* EGFR-targeted immunoliposomes as a selective delivery system of simvastatin, with potential use in treatment of triple-negative breast cancers. *Int J Pharm.* 2019;569:118605,1-14.
DOI: 10.1016/j.ijpharm.2019.118605.